Optimum Vibration Angle for Transporting Granular Materials on Linear Conveyors

James Nyambega Keraita[1,#]

1 Department of Mechanical Engineering, Jomo Kenyatta University of Agriculture and Technology, 62000-00200 Nairobi, Kenya
Corresponding Author / E-mail: keraitajn@eng.jkuat.ac.ke, TEL: +254 67 52711, FAX: +254 67 52164

KEYWORDS : Linear vibratory conveyors, Granular matter, Point mass model, Sliding and hopping, Optimum vibration angle

Vibratory conveyors are widely used in industry to transport granular materials and products. A theoretical point mass model for vibratory conveying was studied. The results agreed well with experimental observations. The model theory included the resting, sliding and flight states of the material. Each state was considered separately when determining the equations of motion. For the coefficients of restitution, values of zero for the normal component and 0.8 for the tangential component were found to be appropriate for modeling the collisions of the granular particles with the conveying surface. The vibration angle had a large influence on the mode and rate of transport. There was an optimum vibration angle for a given set of conditions. The optimum vibration angle decreased and was better defined as the coefficient of friction increased. The results suggest the existence of an optimum dimensionless track acceleration (throw number), which does not support general industrial practice in which the track acceleration is limited when the feed cycle becomes erratic and unstable.

Manuscript received: July 25, 2007 / Accepted: December 18, 2007

NOMENCLATURE

A_0 = amplitude of vibration
x_m = distance of mass body m in the x direction
y_m = distance of mass body m in the y direction
a_n = limiting normal acceleration
g_n = normal acceleration due to gravity
α = inclination angle to the horizontal
β = angle of projection
ε_n = normal coefficient of restitution
ε_t = tangential coefficient of restitution
Γ = throw number
φ = vibration angle
μ = coefficient of friction
ω = circular frequency (angular velocity)

1. Introduction

It is rarely possible to economically replace the transport of small parts by vibratory conveyors in industrial production lines using any other technology. Linear conveyors are particularly advantageous when individual parts must be separated from a group and fed at a controlled rate into an assembly, or into inspection, weighing, or packaging equipment. Therefore, it is worthwhile to determine the optimal operating conditions of such conveyors. Vibratory conveyors may be driven by an electric motor with a fixed eccentric shaft (or rotating weight) or an electromagnet. The generated vibrations are then controlled to create circular, elliptical, or linear movement. Linear vibration is usually desired, especially for conveying and screening purposes. Elliptical motion is used to drive screens, packers, shakeouts, or bin-dischargers. For pure conveying purposes, circular drives do not have many applications except in annular conveyors.

Recently, the study of dry granular matter on vibratory conveyors has attracted renewed interest due to its technological relevance in industrial applications.[1-4] A granular material is defined as a conglomeration of discrete solid macroscopic particles characterized by a loss of energy whenever the particles interact. The constituents that compose granular materials must be large enough that they are not subject to thermal motion fluctuations. Thus, the lower size limit for grains in granular material is about 1 μm. For the upper size limit, the physics of granular materials may be applied to ice floes where the individual grains are icebergs. As transport phenomena involve nonlinear interactions of multiparticle systems and the individual particles are irregular in shape, volume, and density, the investigation of vibrating granular materials is a challenging subject. Determination of the precise transport rate is even more difficult.

This paper presents a dynamic analysis of moving parts on a linear vibratory conveyor. A combination of computational and experimental analyses was used to investigate the effects of vibration angle on the transport rate of granular materials with the aim of determining an optimum value. The use of an optimum vibration angle will greatly enhance the performance of devices such as automatic combination weighers, where the vibrating line feeders are required to supply a given amount of products (at high speed) to hoppers for weighing, combination, and selection operations for each cycle. With better combination algorithms[5,6] and advanced sensor technologies and software techniques,[7,8] efforts are now being directed toward improving the transport rate to increase the number of

weight measurements performed per minute.

2. Theoretical Background

2.1 Model and Analysis of Forces Affecting Motion

Theoretical methods for determining the optimal vibratory conveying conditions are becoming important. For example, MacDonald and Stone[9] developed a simple linear vibratory feeder model using MacPascal, while Lim[10] used Turbo C++. Berkowitz and Canny[11] developed a model for performing parameter enumeration, analyses, and Markov model building of part feeders using dynamic impact simulation. However, most previous studies have been restricted to the sliding transport mode. More recently, Han and Lee[12] used frictional impact analysis theory to describe the dynamics of vibratory conveying in bowl feeders operating in hopping mode. The results showed that the hopping regime can be classified into periodic and chaotic regions, which can be identified by numerical simulation and experimental analysis.

Figure 1 shows a part on a straight vibrating plate that is inclined at a small angle to the horizontal. The plate is at the upper limit of its motion. This forms the basis of the model considered in this research and contains appropriate modifications to an earlier approach proposed by Boothroyd[13] to include a detailed study of the hopping regime.

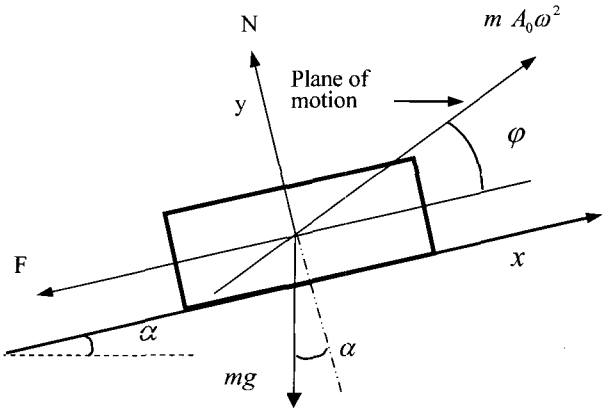

Fig. 1 Forces acting on a part during vibratory feeding

We assume that the forcing mechanism provides a simple harmonic motion, the motion of the part is independent of its shape, and the mass of the plate is much greater than the mass of the part, m. Thus, the dynamic motion of the plate is unaffected by the part during the process. Factors that could affect the rigid body conveying velocity include the angle of vibration, φ, amplitude of the plate vibration, A_0, coefficient of friction, μ, inclination of the plate to the horizontal, α, and the operating frequency, ω. These factors were incorporated in our analyses.

For small amplitudes, the part will remain stationary on the plate because the acting parallel inertia force will be too small to overcome the frictional resistance, F, between the part and the plate. By analysis of forces, the conditions required for forward and backward sliding to occur during the vibration cycle are

$$\text{Forward sliding:} \quad \frac{a_n}{g_n} > \frac{\mu + \tan\alpha}{\cot\varphi + \mu} \tag{1}$$

$$\text{Backward sliding:} \quad \frac{a_n}{g_n} > \frac{\mu - \tan\alpha}{\cot\varphi - \mu} \tag{2}$$

where a_n is the limiting normal plate acceleration and g_n is the normal acceleration due to gravity. The dimensionless normal plate acceleration a_n/g_n is given by

$$\frac{a_n}{g_n} = \frac{A_0\,\omega^2 \sin\varphi}{g\cos\alpha} \tag{3}$$

For example, for values of $\mu = 0.75$, $\alpha = 2.5°$, and $\varphi = 25°$, the ratio a_n/g_n must be greater than 0.274 for forward sliding to occur and greater than 0.507 for backward sliding to occur. Thus, if the ratio is say 0.4, the part will start to slide forward at some instant when the plate approaches the upper limit of its motion, but it will not slide backwards at any instant during the vibration cycle. If the ratio is 0.6, backward sliding will occur during the vibration cycle after a period of forward sliding. Backward sliding is likely to occur when the plate approaches the lower limit of its motion. The ratio a_n/g_n is often referred to as the throw number (Γ).

At sufficiently large vibration amplitudes, the part can leave the plate and travel in free flight. This occurs when the y component of the acceleration becomes greater than gravity in the same direction. This condition is equivalent to the normal reaction, N, between the part and the plate becoming zero. The part will leave the plate during part of the vibration cycle if

$$\frac{a_n}{g_n} = \Gamma \geq 1 \tag{4}$$

Figure 2 shows a graphical illustration of the limiting conditions for the various modes of conveying for $\mu = 0.75$ and $\alpha = 2.5°$. Backward sliding can be avoided during the vibration cycle by employing large vibration angles, but this does not necessarily translate into high forward conveying rates. The velocity and inclination of the part to the plate at the start of the free flight each have a large influence on the conveying rate.

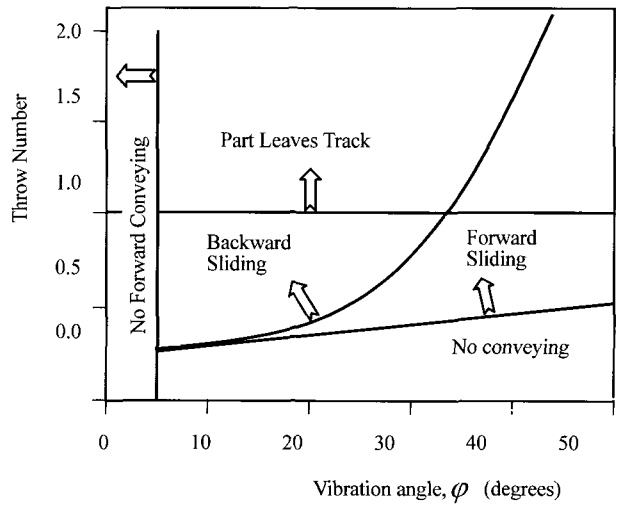

Fig. 2 Limiting conditions for various modes of vibratory conveying

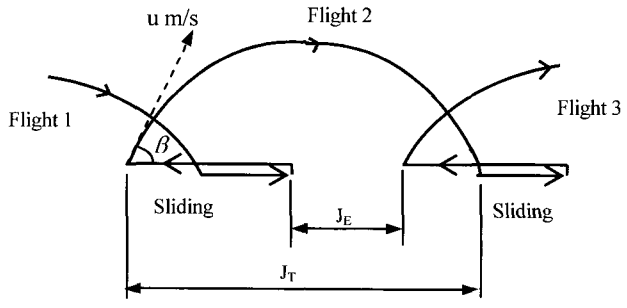

Fig. 3 Typical motion sequence while hopping

Figure 3 shows a typical motion sequence. Clearly, as the backward sliding time increases (a condition favored by small

vibration angles), the effective hop J_E is diminished. If the projection angle β increases above 45°, the total hop J_T diminishes even though the part spends more time in free flight. Consequently, the effective hop will be reduced, even if there is no backward sliding. The total

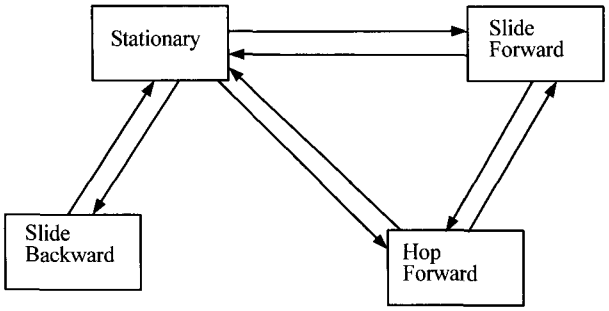

Fig. 4 The state of motion diagram

hop is reduced with increases in the vibration angle[13] mainly due to the corresponding increase in the projection angle. Thus, there exists an optimum vibration angle for a given set of conditions.

After free flight, a number of distinct types of motion (see Fig. 4) are possible, depending on the local plate conditions at the point of impact and the impact velocity. We successively analyzed the distinct types of motion as they occurred and determined the transport rate from the mean values of velocities along the plate over several cycles of the conveying process.

2.2 Phase of Motion Analysis

2.2.1 Resting and Sliding Phases

The equations of motion of the body on the plate are

$$\left.\begin{aligned} m\ddot{x}_m &= -mg\sin\alpha \mp F \\ m\ddot{y}_m &= N - mg\cos\alpha \end{aligned}\right\} \tag{5}$$

The negative or positive signs for the frictional force, F, are used to indicate sliding in the positive or negative x direction, respectively. The subscript m indicates the body, which is considered as a point mass. For both resting and sliding cases,

$$\ddot{y}_m = \ddot{y}_p \tag{6}$$

Using Eqs. (3) and (5), the dimensionless acceleration of the body during the sliding phase is

$$\ddot{X}_m(t) = \tan\varphi\left[\frac{1}{\Gamma}(\mp\mu - \tan\alpha) \pm \mu\sin\omega t\right] \tag{7}$$

Recall that

$$\left.\begin{aligned} X(t) &= \sin\omega t \\ \dot{X}(t) &= \cos\omega t \\ \ddot{X}(t) &= -\sin\omega t \end{aligned}\right\} \tag{8}$$

Sliding starts when the acceleration of the mass and trough are equal. This occurs when

$$\sin\omega t = \pm\frac{1}{\Gamma}\frac{(\mu \pm \tan\alpha)\tan\varphi}{1 \pm \mu\tan\varphi} \tag{9}$$

Similar equations were derived by Sloot and Kruyt.[1] The velocity of the point mass can be obtained by integrating Eq. (9) with respect to time. The boundary condition states that the velocities of the point mass and plate are equal at the start of a positive or negative sliding phase. A second integration yields the dimensionless relative displacement.

2.2.2 Flight Phase and Collisions

A flight phase occurs if the normal force N becomes zero. The motion is similar to that of a projectile. At the start of flight, the mass and plate have the same y coordinate and y velocity. Using Eq. (5) and the y counterparts of Eq. (8), it follows that the flight phase starts at

$$\omega t = \sin^{-1}\left(\frac{1}{\Gamma}\right) \tag{10}$$

The end of flight can be derived from the condition of equal y coordinates. The tangential acceleration acting on the point mass remains equal to

$$\ddot{x}_m = -g\sin\alpha$$

or

$$\ddot{X}_m = -\left(\frac{1}{\Gamma}\right)\tan\alpha\tan\varphi \tag{11}$$

The velocity of the point mass can be determined by integrating this expression and applying a boundary condition consisting of a known tangential velocity at the end of the flight. The tangential velocity can be determined from the movement phase that occurred before the flight. The relative displacement can then be obtained through a second integration.

Collisions of the mass with the plate are assumed to be inelastic and instantaneous. Hence, the normal and tangential velocities of the mass directly after a collision can be related to the corresponding velocities directly before the collision via the tangential and normal restitution coefficients, ε_t and ε_n,

$$\left.\begin{aligned} \dot{x}_{m,i} &= \varepsilon_t\,\dot{x}(t_i) \\ \dot{y}_{m,i} &= \varepsilon_n\,\dot{y}(t_i) \end{aligned}\right\} \tag{12}$$

Here, t_i denotes the impact time of the mass and the plate. The restitution coefficients account for the energy loss of the block at impact and can take on arbitrary values between 0 and 1.

3. Experimental Setup and Procedures

One of the channels was disassembled from a previously developed automatic combination weigher and used for the experimental investigation. Figure 5 shows a photograph of the line feeder together with the in-feed circular feeder and hoppers. The vibrating line feeder consisted of a base member below a spring-supported trough (pan). During operation, the drive transmitted vibrations through the support springs to the trough. The generated vibrations were controlled to create a linear movement. The conveying surface consisted of a polished flat steel plate, and the conveyed components were small self-tapping screws, each weighing about 2.5 g.

First, the physical parameters were determined in order to carry out the theoretical analysis. In the tests, the vibration amplitude of the trough was varied by adjusting the input voltage to the driving unit while maintaining the operating frequency at 60 Hz. The horizontal ($\alpha = 0$) trough was driven sinusoidally in time. Although it has been shown that improvements in the transport rate can be obtained by inclining the conveyors at small negative angles[1], the results presented are only for the sliding case. Theoretical explanations do not envisage this phenomenon to extend to the hopping regime.

The vibration angle was determined experimentally using accelerometers and was altered by adjusting the mounting angle of the vibrodriver. As the vibration frequency was fixed, the vibration amplitude A_0 for each input voltage and the corresponding throw number Γ could be calculated. The coefficient of friction was

determined by common laboratory procedures[13] and the velocity was measured by tracking a colored part that was carried along with the bulk screws. Due to setup difficulties, the velocity was not measured for a case with net backward motion. Several repetitions were necessary to yield valid average values for the coefficient of friction as well as the conveying velocity.

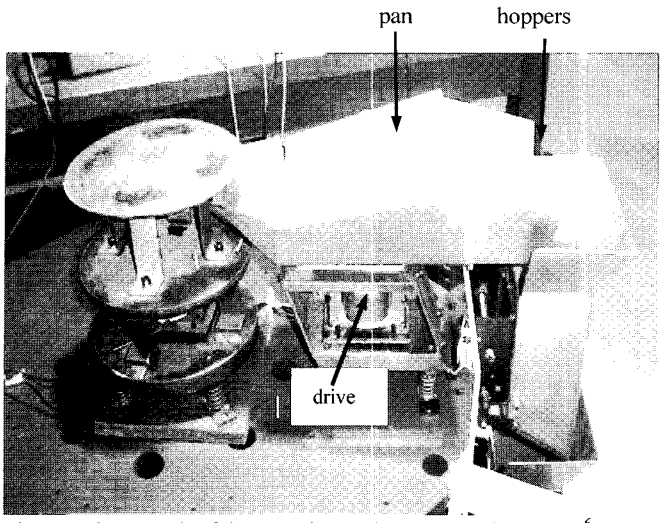

Fig. 5 A photograph of the experimental setup (also in Keraita[6])

4. Results and Discussion

4.1 Coefficient of Restitution

Modeling impacts can be a difficult task. We set the normal component of the restitution coefficient to zero, which suggests that parts being conveyed did not bounce. However, bouncing normally occurs in practice at very high track accelerations and leads to undesirable wear and damage of the parts as well as an erratic transportation mode. The approach we used to determine a suitable value for the tangential component of the restitution coefficient was to present theoretical results for high, moderate, and low energy losses (*i.e.*, ε_t = 0.2, 0.5, and 0.8), and then compare them with experimental data. The computations followed the equations developed in Section 2.2. The theoretical results for the three restitution coefficients were essentially the same before the hopping regime commenced ($\Gamma \geq 1$).

Figure 6 shows the results obtained for a practical vibration angle of 25° at an experimental coefficient of friction of μ = 0.35. In the figure, the mean conveying velocity was normalized by dividing by the driving velocity, $A\omega \cos \varphi$. A value of ε_t = 0.8 best modeled the impacts. The results revealed a sharp fall in the mean conveying velocity at Γ = 4.5, thought to be mainly due to the parts landing on the trough as it approached its lower limit of motion in successive cycles, leading to considerable backward sliding. A similar phenomenon was observed by El hor and Linz[4] in their study of an annular vibratory conveyor. At $\Gamma \geq 6.0$, the theoretical predictions began to differ significantly from the experimental results, which became rather erratic. These results suggest that there is an optimum throw number that should be used, as opposed to the general industrial practice of operating the conveyors at high track accelerations as long as the feeding cycle is stable.

4.2 Optimum Vibration Angle

The average coefficient of friction determined from the experiments was 0.35. However, the experimental coefficient of friction is prone to considerable error. Therefore, the calculated mean conveying velocity for two other coefficients, μ = 0.25 and 0.60, are presented in Fig. 7. This serves to reveal any trend in the variation of the optimum vibration angle with the coefficient of friction. No distinction was made between the static and kinetic coefficients of friction when calculating the conveying velocities. All results are presented for a practical maximum normal trough acceleration with a throw number of Γ = 1.8.

Figure 7 indicates that the optimum vibration angle decreased and became more defined as the coefficient of friction increased. As expected, an increase in friction led to an increase in conveying at different throw numbers

Figure 8 shows the calculated conveying velocities with vibration

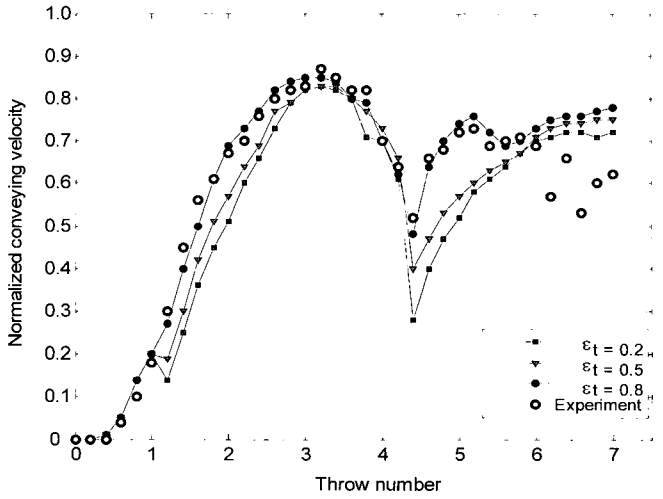

Fig. 6 Variation of the normalized mean conveying velocity with throw number

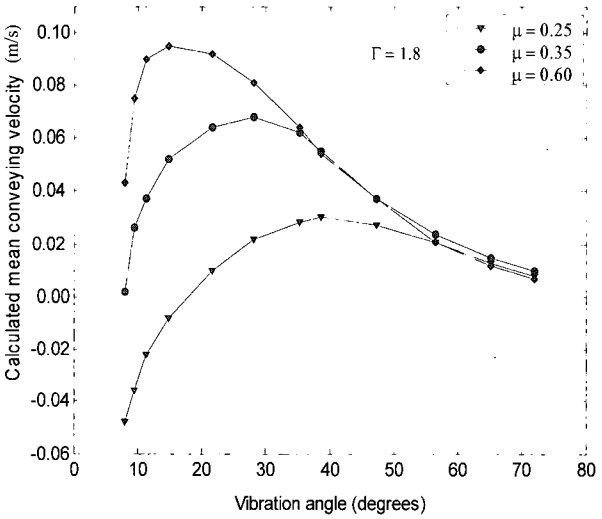

Fig. 7 Variation of the mean conveying velocity with vibration angle at different coefficients of friction

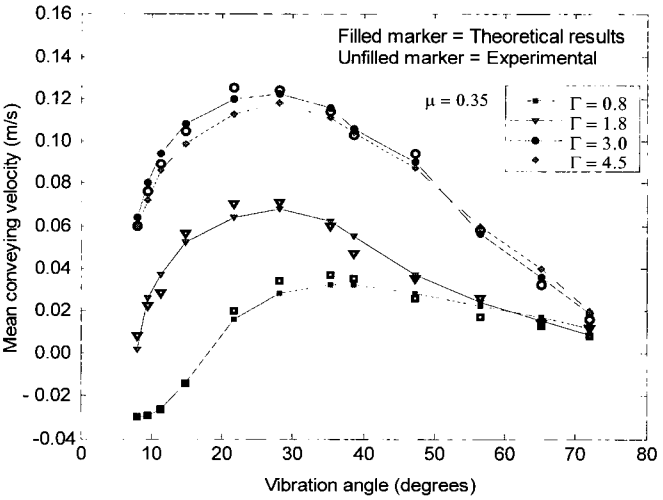

Fig. 8 Variation of the mean conveying velocity with vibration angle velocity

However, this trend was lost at high vibration angles angle at the experimentally determined coefficient of friction ($\mu = 0.35$) for different throw numbers. Theoretical results for $\Gamma = 4.5$ are shown without supporting experimental data for clarity; the data were very similar to the case of $\Gamma = 3.0$. The results show that the optimum vibration angle did not vary much with the throw number. An increase in the coefficient of friction or in the throw number ceased to have a significant effect on the conveying velocity at very high vibration angles.

5. Conclusions

A theoretical point mass model was used to predict the mean conveying velocity of granular matter on linear vibratory conveyors for both sliding and hopping modes of transport. The vibration angle had a large influence on the mode and rate of transportation, and this should be taken into account when designing conveyors. There existed an optimum vibration angle for a given set of conditions. This optimum vibration angle remained fairly constant over a wide range of practical throw numbers.

The transport rate did not increase monotonically with the throw number during the hopping mode, where the conveying velocity was generally high. These results suggest that the conveyor should be operated at an optimum throw number, as opposed to the general industrial practice of operating the conveyors at high track accelerations as long as the feeding cycle is stable. Factors such as power consumption and wear and damage of the parts must be taken into consideration when determining the optimum throw number.

REFERENCES

1. Sloot, E. M. and Kruyt, N. P., "Theoretical and experimental study of the transport of granular materials by inclined vibratory conveyors," Powder Technology, Vol. 87, No. 3, pp. 203-210, 1996.
2. Grochowski, R., Walzel, P., Rouijaa, M., Kruelle, C. A. and Rehberg, I., "Reversing a granular flow on a vibratory conveyor," Applied Physics Letters, Vol. 84, No. 6, pp. 1019-1021, 2004.
3. Kruelle, C, A., Götzendorfer, A., Rehberg, I., Grochowski, R., Rouijaa, M. and Walzel, P., "Granular flow and pattern formation on a vibratory conveyor," Proceedings of Traffic and Granular Flow, pp. 111-128, 2005.
4. El hor, H. and Linz, S. J., "Model for transport of granular matter on an annular vibratory conveyor," Journal of Statistical Mechanics, L02005, pp. 1-8, 2005.
5. Keraita, J. N. and Kim, K. H., "A weighing algorithm for multihead weighers," International Journal of Precision Engineering and Manufacturing, Vol. 8, No. 1, pp. 21-26, 2007.
6. Keraita, J. N. and Kim, K. H., "A study on the optimum scheme for determination of time of operation of line feeders in automatic combination weighers," Journal of Mechanical Science and Technology, Vol. 20, No. 10, pp. 1567-1575, 2006.
7. Brignell, J. E. and White, N. M., "Intelligent Sensor Systems," Inst. of Physics, pp. 56-117, 1994.
8. Keay, M., "Improving the multihead," Machinery Update, pp. 38-42, 2005.
9. MacDonald, S. A. and Stone, B. J., "An investigation of vibratory feeders," In Proc. Int. Conf. of Noise and Vibration, pp. C12-C26, 1989.
10. Lim, G. H., "On the conveying velocity of a vibratory feeder," Computers and Structures, Vol. 62, No. 1, pp. 197-203, 1997.
11. Berkowitz, D. R. and Canny, J., "Designing parts feeder using dynamic simulation," Proceedings of IEEE International Conference on Robotics and Automation, pp. 1127-1132, 1996.
12. Han, I. and Lee, Y., "Chaotic dynamics of repeated impacts in vibratory bowl feeders," Journal of Sound and Vibration, Vol. 249, No. 3, pp. 529-541, 2002.
13. Boothroyd, G., "Assembly Automation and Product Design," Marcel Dekker, p. 33, 1992.